



Properties of Plastic Composites Filled with Giant Reed Flour and Magnesium Oxide Nanoparticles

Nadir Ayırlımış ^a, Elif Yurttaş^a, Esra Yıldız Avsar^a, Memet Vezir Kahraman ^b,
Ferhat Özdemir^c, Sivasubramanian Palanisamy^{d,*}, Ferhat Yetiş^e,
Madhan Kumar Gurusamy^f and Saleh A Al-Farraj^g

Wood plastic composites (WPCs) were produced from recycled polypropylene (RPP) matrix, giant reed (GR) flour, and magnesium oxide nanoparticles (nano-MgO). The physical, mechanical, and thermal properties were analyzed. Different amounts of GR flour from 10 wt% to 40 wt%, and nano-MgO from 1.0 wt% to 2 wt% were added into the RPP matrix. The water resistance, mechanical, and thermal properties of the injection molded WPCs were determined according to the ISO standards. The bending and tensile modulus of the WPCs were considerably enhanced with the addition of the GR flour up to 40 wt%, while this was found to be maximum at 30 wt% for the bending and tensile strengths. The water absorption of the WPCs increased with the addition of the GR flour, as expected. The results of thermal analysis revealed that the addition of the GR flour increased the thermal stability of the WPCs, especially the degree of crystallization and the melting enthalpies of the RPP matrix, due to the good adhesion between the GR flour and the RPP. The incorporation of the nano-MgO affected adversely the mechanical properties of the WPCs. Lower thermal stability was observed for WPCs containing nano-MgO. The inclusion of 30 wt% GR flour in the RPP matrix gave the best mechanical and thermal properties.

DOI: 10.15376/biores.20.2.2670-2686

Keywords: Reed fiber; Thermoplastic; Polymer composites; Magnesium oxide; Mechanical properties; Water absorption

Contact information: a: Department of Wood Mechanics and Technology, Faculty of Forestry, Istanbul University-Cerrahpasa, Istanbul, Türkiye; b: Department of Chemistry, Faculty of Science, Marmara University, 34722 Istanbul, Türkiye; c: Department of Wood Chemistry and Technology, Faculty of Forestry, Kahramanmaraş Sutcu Imam University, 46100, Kahramanmaraş, Türkiye; d: Department of Mechanical Engineering, P T R College of Engineering & Technology, Thanapandiyar Nagar, Austinpatti, Madurai-Tirumangalam Road, Madurai, 625008, Tamilnadu, India; e: Marmara Forestry Research Institute, 34485, Sariyer, Istanbul, Türkiye; f: Department of Aeronautical Engineering, Sathyabama Institute of Science and Technology, Chennai, Tamilnadu, India; g: Department of Zoology, College of Science, King Saud University, Riyadh 11312, Saudi Arabia;

* Corresponding author: sivarsearch948@gmail.com

INTRODUCTION

Arundo donax L., also known as the giant reed (GR), has been spreading unchecked in many parts of the world. In particular, the International Union for the Conservation of Nature has ranked giant reed (Fig. 1) as one of the 100 most dangerous invasive species in the world (Suárez *et al.* 2021). This can be attributed to its rapid growth, its pyrophoric nature, and the contribution it makes to spreading fire. The GR plant is adaptable to different climatic conditions and is easy to grow. It can yield very high biomass per unit

area because it can be harvested every year. It is widely distributed in Mediterranean countries and is a perennial plant species that can grow in different ecological conditions. The giant reed is a suitable crop for the purpose of the energy production due to the high biomass yield that is capable of reaching 37.7 tonnes of dry matter per hectare per year (Angelini *et al.* 2009). The adult stem is hollow and about 2 cm in diameter. The leaves, which can grow up to 60 cm, are 2 to 6 cm wide (Monteiro *et al.* 2015). When suitable climatic and growing conditions occur, it can be harvested between 7 and 12 months (Arslan and Şahin 2014). Because it has a hollow structure like bamboo, it can be used for various purposes, such as tomato and bean poles in greenhouses, roofing, partition walls, *etc.*, in village houses. The high cellulose content of the GR plant and its fibrous properties are similar to those of hardwoods. Thus it can be used as an alternative lignocellulosic raw material to wood, and it is valuable for the wood-plastic composites (WPC) industry (Arslan and Şahin 2014).

Although the GR plant is an herbaceous plant, its chemical structure consists of holocelluloses (cellulose, hemicellulose), lignin, and extractives. The main components of the GR are similar to those of the wood. The amount of these constituents ranges between tree species. The proportions for wood are 40 to 50 wt% cellulose, 20 to 30 wt% lignin, and 25 wt% to 35 wt% hemicellulose (Ayrilmis and Ashori 2014; Ayrilmis *et al.* 2024; Palaniappan *et al.* 2024). The amounts of the cellulose, hemicellulose, and lignin of the GR have been reported as 40 to 45 wt%, 20 to 25 wt%, and 20 to 25 wt%, respectively (Licursi *et al.* 2015). The GR plant contains less cellulose and lignin but it contains a proportion of extractives (Arslan and Şahin 2014). The average fiber length and width of coniferous wood is 3.3 mm and 33 µm, respectively, whereas the average fiber length and width of hardwood is 1 mm and 20 µm, respectively (Lilholt and Lawther 2000). In contrast, the fiber length and width of the GR plant are approximately 1.2 mm and 17 µm, respectively (Arslan and Şahin 2014). In terms of fiber properties, the GR plant fibers are like hardwood fibers. Based on the literature, alternative lignocellulosic sources, such as annual plants, agricultural crops, and dangerous invasive species, have been investigated as fillers in thermoplastic composites due to the annual decrease in wood raw material. Many countries are focusing on the use of their own indigenous plant fibers as an alternative to wood in the production of the WPC. The effects of different lignocellulosic sources on the properties of synthetic thermoplastics have been extensively studied, for example, kenaf fibers (Pan *et al.* 2007), sisal (Alvarez *et al.* 2003), bamboo (Meng *et al.* 2023), jute (Plackett *et al.* 2003), walnut shell (Ayrilmis *et al.* 2013), sunflower stalk (Kaymakçı *et al.* 2013), and waste paper (Huda *et al.* 2005). In many of these studies, the addition of lignocellulosic fillers to thermoplastics was found to significantly increase the tensile and flexural modulus of elasticity because the modulus of lignocellulosic materials, such as wood, flax, and hemp, is higher than that of many thermoplastics such as HDPE and polypropylene. Moreover, bending strength of thermoplastics filled with lignocellulosics increased to some extent, while impact strength is reduced (Feng and Xie 2021; Sumesh *et al.* 2024).

Recently, high value-added metal oxides, such as zinc oxide, magnesium oxide, titanium oxide, and silicon dioxide, have been incorporated into various types of thermoplastics to impart specific properties such as good thermal stability and strength properties (Huda *et al.* 2005; Kiaei *et al.* 2017; Mashkour and Ranjbar 2018; Basalp *et al.* 2020; Feng and Xie 2021; Durmaz *et al.* 2023). Of these metal oxides, magnesium oxide (MgO) nanoparticles, have recently attracted attention as an environmentally friendly, economical, and industrially valuable material (Kiaei *et al.* 2017). MgO is an inorganic

material with a molecular weight of 40.31 g/mol and a density of 3.58 g/cm³ (Hornak 2021). The most important properties of the nano-MgO are structural strength, chemical stability, biological durability, fire resistance, dielectric strength, and optical transparency (Kiaei *et al.* 2017; Hornak 2021; Gatou *et al.* 2024). MgO, a crystalline mineral, is used in a wide range of applications, such as adsorbents, fire retardants, advanced ceramics, toxic waste remediation, photoelectronic materials, and refractory materials (Kiaei *et al.* 2017; Adhikari *et al.* 2021; Hornak 2021; Gatou *et al.* 2024).

A literature review revealed that although some of the technological properties of paper, wood-based panels, and polymer composites containing GR plant have been previously investigated (Shatalov and Pereira 2006; García-Ortuño *et al.* 2011; Fiore *et al.* 2014; Ramos *et al.* 2018; Suárez *et al.* 2022, 2024), the combined effect of the GR flour and nanofillers, in particular nano metal oxides, on the thermoplastic composites has not yet been investigated. This study aimed to improve the mechanical and thermal properties of thermoplastic WPCs filled with GR flour and the nano-MgO. The main properties, such as bending and tensile behavior, thermal stability, and water absorption, of the WPCs were investigated.

EXPERIMENTAL

Materials

The GR plants with lengths ranging from 1.0 m to 1.5 m and diameters averaging 2 cm were kindly supplied from Aegean Forestry Research Institute, Izmir, Turkey. First, the reeds were turned into coarse chips in a laboratory type using a laboratory type chipper machine with three knives. Following this process, the chips were laid on plastic cloth for about a week and allowed to reduce their moisture content. The chips were ground in a laboratory type mill to turn them into particles for the WPC production. The small reed particles were sieved for 10 min, and the particles passing through the 0.237-mm sieve openings were used in the experiments. Before the compounding process, the particles were dried to less than 1% moisture content at 100 °C for 3 h.



Fig. 1. Giant reed (GR) (*Arundo donax* L.) samples

The RPP matrix was purchased from a plastic recycling company (Eforkim Company Istanbul, Turkey). It had a melt flow index (MFI) of 6.54 g / 10 min (2.16 kg / 230 °C) and a density of 0.90 g/cm³. Nano-MgO with a specific surface area of 126 m²/g was supplied by Grafen Nanotechnology Company, Ankara, Turkey. The average crystallite size of the nano-MgO was 25 nm. It was in disc form with a diameter of 40 nm to 60 nm and thickness of 5 nm.

Preparation of Injection Molded Polymer Composites

The required amounts of the reed particles, nano-MgO, and RPP granules of each formulation were mixed according to Table 1. Before compounding in the extruder, the raw materials were uniformly pre-mixed. The mixture was fed into the volumetric feeder of the co-rotating twin screw extruder. The heating temperature in the extruder barrel from the inlet to the exit was between 180 and 190 °C at a screw speed of 40 rpm. The residence time of the compound in the extruder was about 2 min. The composite filaments were cooled in a water bath and then pelletized using a pelletizer. The pellets were dried to 1% in an oven were put in the feeder of the injection molding machine. The pellets were injected into the mold at 170 to 190 °C (from inlet to the exit) and 4 to 5 MPa pressure. Prior to testing, the resulting samples were conditioned in a climatic chamber at 50% relative humidity and 20 °C in accordance with ISO 291 (2008) standard. The raw material compositions of the 4-mm-thick WPCs are displayed in Table 1. The RPP matrix and the WPCs without the nano-MgO were also prepared for comparison with the WPCs containing 1 wt% and 2 wt% contents of the nano-MgO. The density of the WPCs was in the range of 0.98 to 1.04 g/cm³.

Table 1. Experimental Design

Specimen Code	Recycled PP (RPP) (wt%)	GR Flour (wt%)	Nano-MgO (wt%)
A	100	-	-
B	90	10	0
C	80	20	0
D	70	30	0
E	60	40	0
F	89	10	1
G	79	20	1
H	69	30	1
I	59	40	1
J	88	10	2
K	78	20	2
L	68	30	2
M	58	40	2

Water Absorption and Mechanical Characterization of WPCs

Water absorption of the specimens was performed based on the ISO 62 (2008) standard. Ten specimens were immersed in the water bath at 20 °C for 28 days. Then, the water absorption percentage of the specimens was calculated from the initial and final weights. The bending strength (MOR) and bending modulus (MOE) of the WPCs were determined using the ISO 178 (2010) standard on the material tester machine (Lyold instruments Ltd., Bognor Regis, UK). The speed of the moving crosshead of the test machine for the bending properties was 5 mm/min. Ten specimens were used in bending tests. The tensile tests were determined based on the ISO 527-2 (2012) standard. The test

speed of the crosshead was 2 mm/min. Ten specimens were used for the tensile tests. The notched impact strength of the specimens was determined in accordance with ISO 180 (2019). Ten specimens were tested on the 2J impact bending machine (Devotrans Co., Istanbul, Turkey). Prior to the testing, the specimens were conditioned in accordance with the ISO 291 (2008) standard.

Thermogravimetric and Differential Scanning Calorimetry Analysis

Thermal stability of WPCs was determined by a thermogravimetric analyzer (TGA) (Mettler Toledo TGA/SDTA851, Greifensee, Switzerland) under N₂ atmosphere. A small quantity of each specimen (5 to 10 mg) was heated from 25 to 600 °C at 10 °C min⁻¹ heating rate. Thermal stability of the WPCs and the RPP specimens were determined using a differential scanning calorimetric (DSC) analyzer (Mettler Toledo TGA/SDTA851) under N₂ atmosphere. A heating/cooling/heating cycle was performed for the thermal characterisation of WPCs. Approximately 5 mg of samples were heated between 25 °C and 300 °C at 10 °C min⁻¹ heating and cooling rate. The degree of crystallization of the WPCs was calculated using Eq. 1,

$$X_c = \frac{\Delta H_m}{\Delta H_m^0 \omega} \times 100 \quad (1)$$

where X_c is the degree of crystallization (%), ΔH_m is the enthalpy of melting, ΔH_m^0 is the enthalpy of melting of the RPP matrix (207 J g⁻¹) (Črešnar *et al.* 2024), and ω is the weight fraction of the RPP in the WPC.

Morphological Analysis

Fracture surface morphology of the RPP matrix and WPCs was observed using a scanning electron microscope (SEM - JEOL JCM-5000 Neo Scope, JEOL Ltd., Tokyo, Japan). Before SEM observation, the sample surface was sputtered with a thin layer of gold. The SEM was operated at 10 kV acceleration voltage and 5 mm working distance.

RESULTS AND DISCUSSION

Water Absorption

The results of the 28-days water absorption of the WPC specimens are displayed in Fig. 2. The WPCs absorbed more water when the amount of the GR flour was increased in the polymer matrix (Fig. 2). There was no water absorption for the RPP specimens due to its hydrophobic structure. For the WPCs without nano-MgO, the highest water absorption was determined for the specimens with 30 wt% of the GR flour. However, this was not observed for the WPCs with the nano-MgO. A sharp increase in the water absorption values was observed when the filler content increased from 30 to 40 wt%. This result was expected because of the hydrophilic nature of the GR flour that has free hydroxyl groups. Because the free hydroxyl groups of cellulose and especially hemicellulose can hold water molecules, when the filler ratio increases, it causes more water molecules to be held. This situation increases the swelling of the composite and water absorption. It is well known that the water absorption of the WPCs is considerably affected by the defects, such as microgaps, fine pores in the interfacial bonding region, which are created during the compounding and injection processes (Chaudemanche *et al.* 2018; Stokke and Gardner

2003). Due to the incompatibility of the polar lignocellulosic filler with the nonpolar polymer matrix, these defects in WPC may increase as the GR flour content increases (Ayrlimis *et al.* 2013; Mysamy *et al.* 2024; Palanisamy *et al.* 2024).

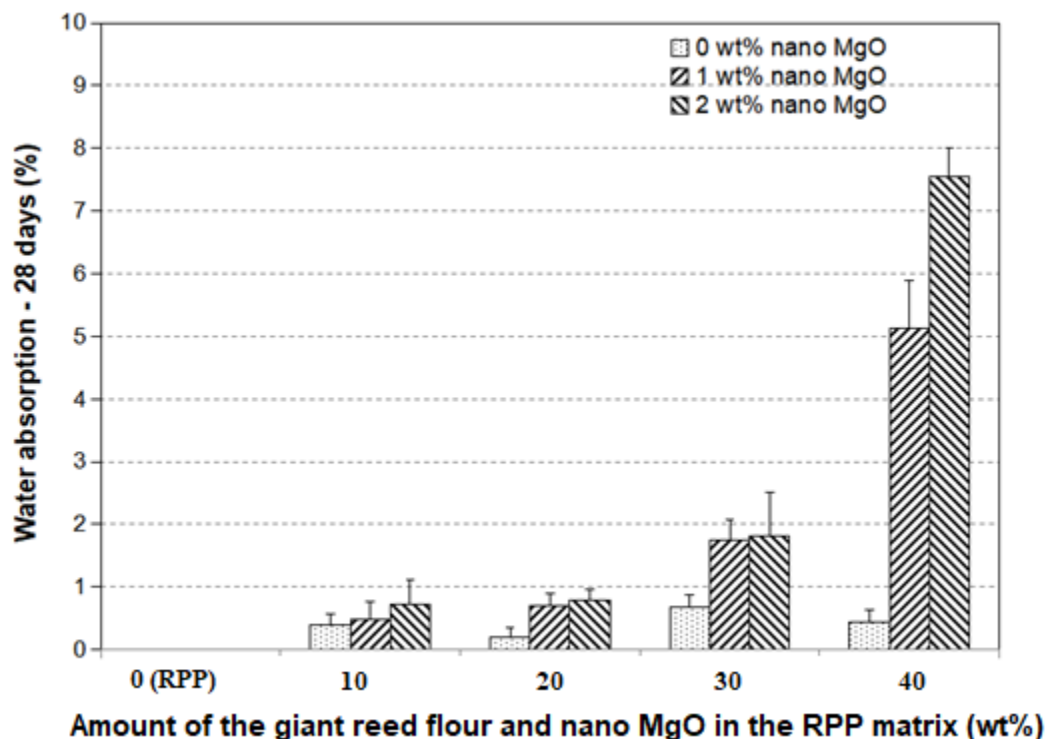


Fig. 2. The water absorption of the WPCs with different amounts of the GR flour and nano-MgO

The addition of the nano-MgO did not decrease the water absorption of the WPCs. In contrast, a considerable increase was observed in the water absorption of the WPCs as compared to the WPCs without nano-MgO. Water absorption values increased as the amount of nano-MgO in the WPC was increased from 1.0 wt% to 2 wt%. This increase was not significant when the ratio of the GR flour was up to 30%, while the water absorption rate increased considerably when the ratio of the GR flour reached to 40 wt%. Macroscopically, the surface of the MgO is hydrophilic and thus nominally strongly interacts with water (Adhikari *et al.* 2021; Hornak 2021). The reason for the higher water absorption of the WPCs containing higher amount of the nano-MgO can be explained by its hydrophilic character.

Mechanical Properties

The results of bending strength of the specimens are presented in Fig. 3. The bending strength of the unfilled RPP specimens was determined to be 42.2 MPa. The addition of the GR flour increased the bending strength. The MOR of the WPCs increased from 57.1 to 75.8 MPa when the amount of the GR flour was elevated from 10 wt% to 40 wt% (35 wt% to 80 wt% increases of the unfilled RPP specimens). The increase in the strength values could be due to an effective load transfer from the polymer matrix to the filler particles as the load transfer occurs along the interface between the filler and the RPP matrix. The tensile strength exhibited a similar trend as the bending strength, as shown in Fig. 4. When GR flour was increased from 10 wt% to 30 wt%, the tensile strength increased

from 31.8 to 35.4 MPa. However, a further increase in the GR flour (40 wt%) reduced the tensile strength. As with the bending strength, the improvement in tensile strength could be partly attributed to the uniform distribution of the GR filler in the RPP matrix, which contributed to a considerable improvement in the stress transfer from the polymer matrix to the filler, thereby increasing the stiffness of the WPC (Ayrilmis and Ashori 2014; Ayrilmis *et al.* 2024). In addition, the filler particles can act as nucleation sites for crack propagation, allowing a more controlled and ductile mode of deformation (Lazzeri *et al.* 2005; Karuppiah *et al.* 2020).

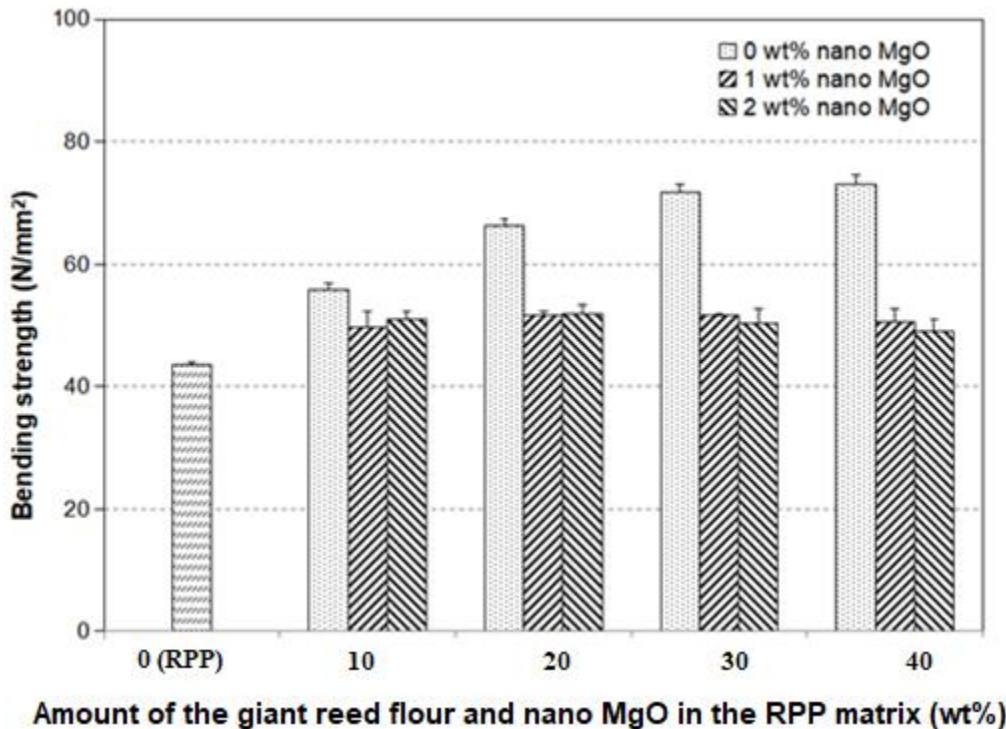


Fig. 3. The bending strength of the WPCs with different levels of the GR flour and nano-MgO

Similar to the strength values, there was also an increase in the modulus values with the increase in the filler content. This ratio of the increase in the tensile and bending modulus was considerably higher than that of tensile and bending strengths. This was due to the increased stiffness of the polymer matrix with the addition of the GR flour (Ezzaraa *et al.* 2023).

The increase in the stiffness of the WPCs can be explained by the high stiffness and rigidity of the GR flour. With increasing stiffness, the amount of energy required for the WPC to undergo elastic deformation increases, which increases the bending and tensile modulus of the WPCs (Figs. 5 and 6). This is mainly due to the reduced amount of the RPP matrix used to bind the filler in the WPC compared to the unfilled RPP specimens. When the RPP matrix melts, it acts as a glue, allowing the GR flour to stick together. In addition, higher wood filler loads of 40 wt% caused wood particles to agglomerate strongly within the RPP matrix, creating zones of stress concentration and reducing the tensile strength.

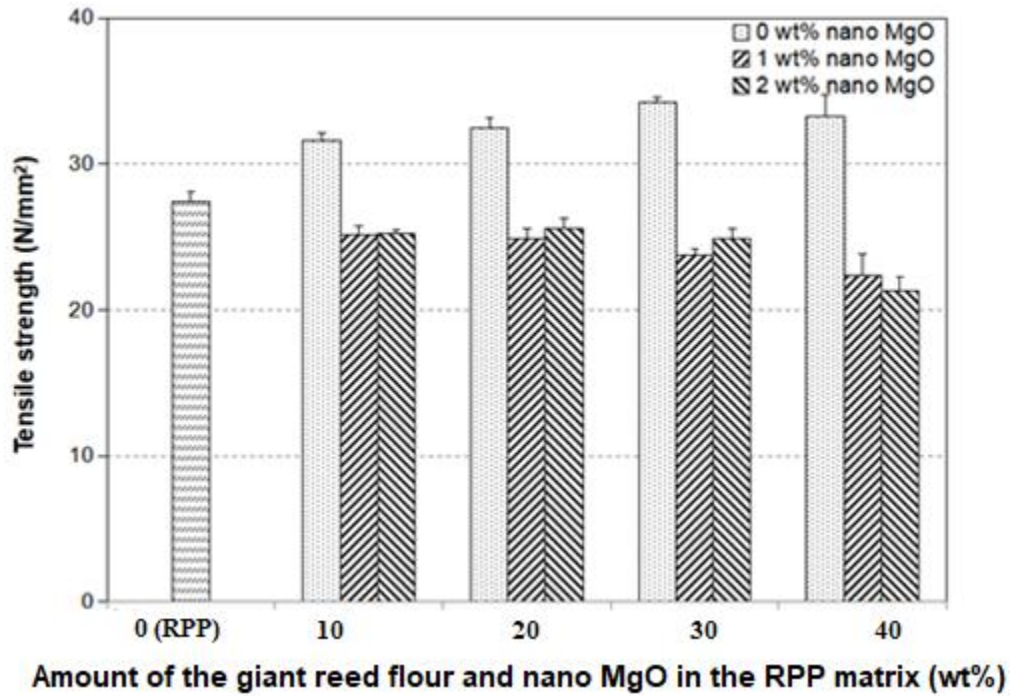


Fig. 4. The tensile strength of the WPCs with different levels of the GR flour and nano-MgO

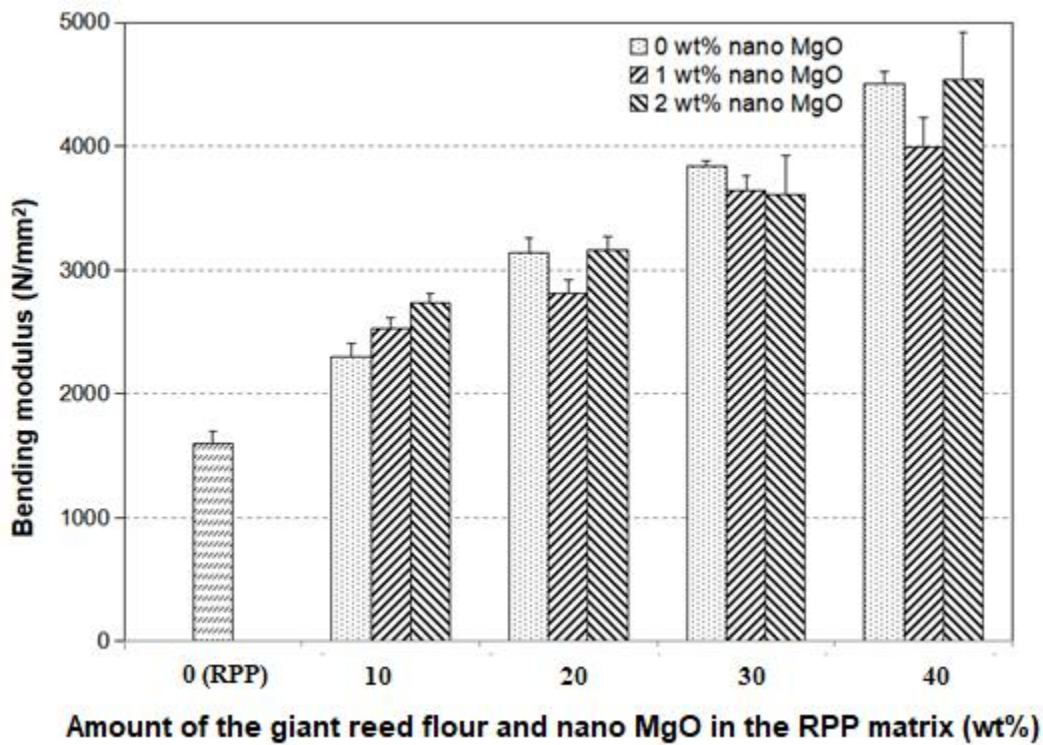


Fig. 5. The bending modulus of the WPCs with different levels of the GR flour and nano-MgO

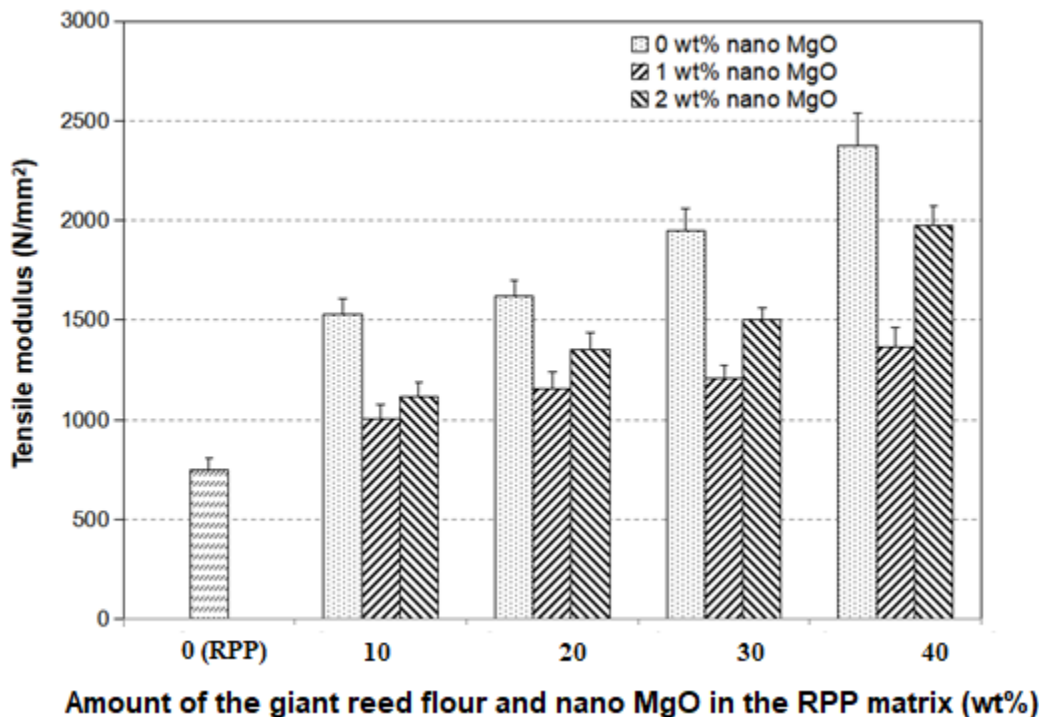


Fig. 6. The tensile modulus of the WPCs with different levels of the GR flour and nano-MgO

According to the test results, a tendency to decrease in the tensile strength was determined when the filler ratio exceeded 30 wt%. This could be due to the fact that the GR flour became highly agglomerated in the polymer matrix, creating stress concentration zones and adversely affecting the tensile and bending performance at higher filler loadings, such as 40 wt%. The agglomeration of the filler particles and the increase in microcavities may explain the fiber pull-out at high filler contents (Ayrilmis *et al.* 2013). However, when 40 wt% filler content was reached, the tensile strength was still higher than that of the WPCs containing 10% and 20 wt% filler content. There was no positive effect of the addition of the 1 wt% and 2 wt% nano-MgO on the strength properties of the WPCs. It was observed that the strength properties of the WPCs with nano-MgO were lower than those of the WPCs without nano-MgO. This may be because of the nano-MgO, which has a high surface area, adversely affects the interfacial adhesion resistance of the polymer matrix and thus stress transfer. A similar result was observed by Durmaz *et al.* (2023). They reported that the addition of nano-ZnO reduced the flexural and tensile strengths of WPCs with a high-density polyethylene (HDPE).

The fracture surface morphologies of the WPCs with and without nano-MgO are shown in Figs. 7a through 7d. The WPCs containing 30 wt% GR flour without nano-MgO showed a rough fracture surface and no pulling out of the GR flour, indicating a good interfacial adhesion between the RPP matrix and the GR filler (Fig. 7a). This could be ascribed to the effective stress-transfer during the tensile testing. However, the holes and de-bounded GR flour can be clearly seen in the SEM photos of the WPCs containing the nano-MgO, which implies a weak interface between the GR and the RPP polymer matrix (Figs. 7b, 7c). The high magnification (Fig. 7d) SEM image of the WPC containing 2 wt% nano-MgO showed the white spots (red arrows), which were likely to the aggregated nano-MgO particles. These nanoparticles could decrease the bonding of the GR flour to the RPP

matrix resulted in a poor interfacial adhesion and the pulling out of the GR from polymer matrix during the tensile testing.

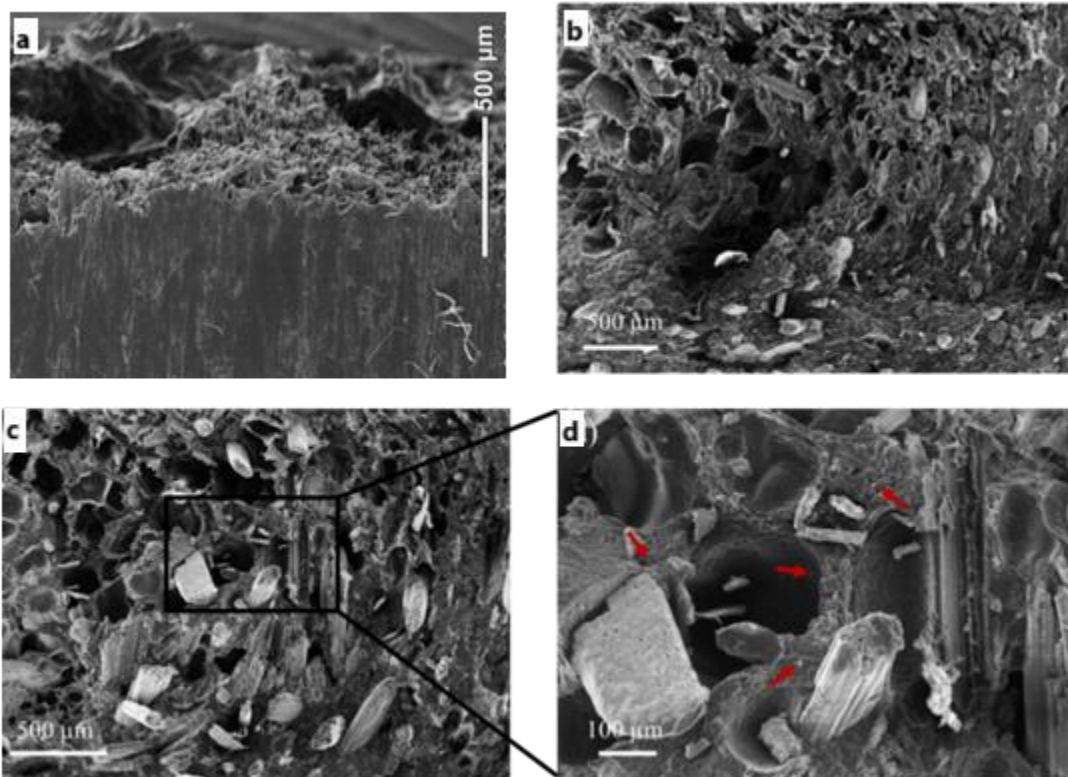


Fig. 7. The SEM images of the fracture surface of the WPCs containing 30 wt% GR flour and 0 wt% nano-MgO (a), 1 wt% nano-MgO (b), and 2 wt% nano MgO (c, d), where (d) is an enlargement from (c)

Thermal Properties

Thermogravimetric analysis

Thermal degradation behaviour of the RPP and WPC groups were determined using TGA analysis. The thermograms indicated the weight loss curves of the WPCs in Fig. 8. The RPP specimens showed a single characteristic thermal decomposition curve of which onset temperature (T_{onset}) was 459 °C. The addition of the GR flour changed the degradation characteristic of the RPP in which a two-step degradation was observed from the TGA thermogram of composites (Fig. 8a). Because the GR flour is a lignocellulosic biomass, the decomposition temperature of their constituents plays a crucial role in the thermal characteristics of final composite materials. Therefore, all WPCs exhibited the first decomposition around 250 °C, which could be attributed to the thermal degradation of the GR flour at a lower temperature compared to the RPP. This could be the overall decomposition of hemicellulose (200 to 300 °C) (Díez *et al.* 2020), cellulose (150 to 400 °C) (Jusner *et al.* 2021), and lignin (105 to 800 °C) (Chen *et al.* 2020), which are the main constituents of GR flour. In the second decomposition, all WPCs displayed a decrease in T_{onset} compared to the RPP matrix, which could be due to the thermal degradation of GR prior to the RPP matrix (Fig. 8a). Moreover, increasing GR content led to a decrease in the T_{onset} of WPCs, which could be the result of the increasing weight fraction of the GR flour into the RPP matrix. The addition of the nano-MgO into the GR flour containing

composites caused a decrease in the T_{onset} and 10 wt% weight loss temperature ($T_{10\%}$) (Figs. 8b and 8c). Perhaps, the nano-MgO negatively influenced the bonding of the polymer as the result of a weak interface through which heat dissipation occurred during the thermal testing of the WPCs. Therefore, the WPCs exhibited better thermal stability compared to the WPCs containing the nano-MgO.

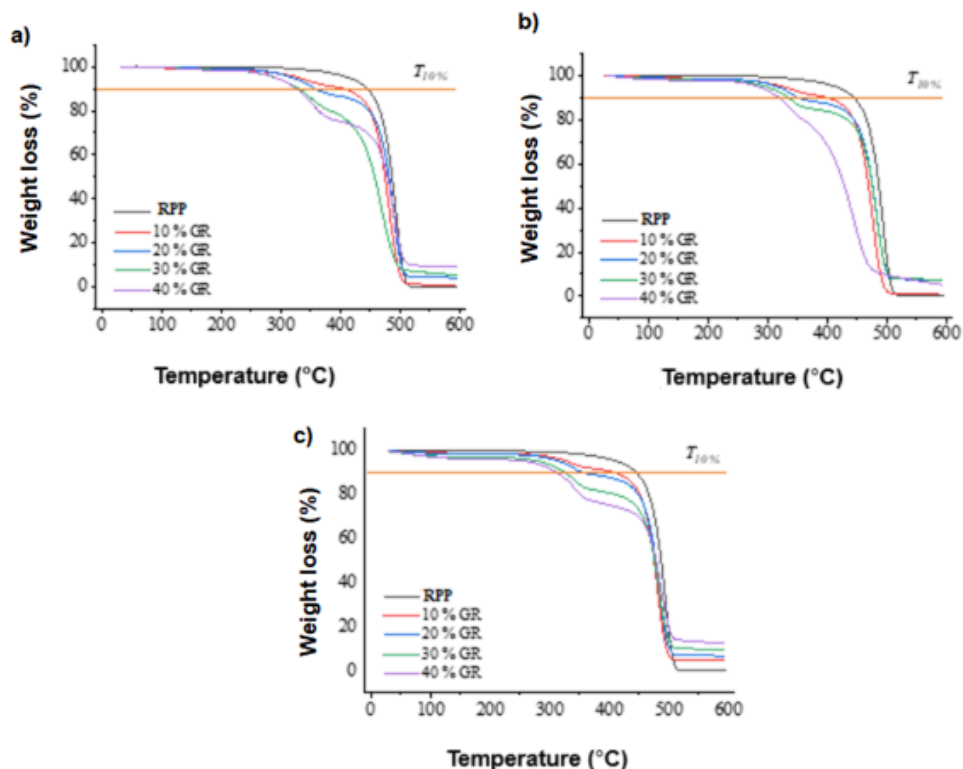


Fig. 8. TGA analysis of the WPCs containing 0 wt% nano-MgO (a), 1 wt% nano-MgO (b), and 2 wt% nano-MgO (c)

Differential Scanning Calorimetric Analysis

Thermal stability of the WPCs containing different concentrations of the GR flour and nano-MgO was measured using DSC analysis. The onset melting temperature ($T_{\text{m onset}}$), melting temperature (T_{m}), crystallization degree (X_{c}), and melting enthalpy (ΔH_{m}) are presented in Table 2. The RPP exhibited a high X_{c} and ΔH_{m} , perhaps resulting from nucleating agent, which could be added during the recycling process of the RPP. Similar results obtained using the same calculation method were presented in previous studies (Lewis *et al.* 2023; Srivabut *et al.* 2023). The addition of the GR flour considerably increased the X_{c} of the RPP, which could be due to the nucleating effect of the GR flour. Further, the increase in the X_{c} of the RPP with the addition of the GR flour could be attributed to a good compatibility between the GR and the RPP (Tisserat *et al.* 2014). The ΔH_{m} of the WPCs reduced with the addition of the GR flour, except for 10 wt% of the GR flour. The incorporation of the nano-MgO led to a remarkable decrease in the X_{c} and ΔH_{m} of the WPCs. This may be due to the poor interface between the nano-MgO and the RPP, preventing the nucleation process for the crystallization of semicrystalline polymer chains. Although nano-MgO alone is a substance with high thermal stability, it is concluded from the test results that the addition of nano-MgO at 2 wt% is probably insufficient to increase

the thermal stability of the WPC. Addition of the nano-MgO above 2% can increase the thermal stability of WPC.

Table 2. DSC Data of the WPCs

Specimen Code	$T_{m\ onset}$ (°C)	T_m (°C)	X_c (%)	ΔH_m (J/g)
A	131.6	160.9	63.3	131.0
B	152.2	162.5	74.9	139.5
C	149.9	160.1	73.1	121.0
D	151.7	161.2	71.8	104.1
E	150.1	162.5	88.5	109.9
F	152.8	161.0	38.2	70.4
G	152.4	160.5	43.3	70.8
H	151.9	161.4	44.0	62.9
I	152.5	160.6	40.0	48.9
J	152.8	160.6	32.0	58.9
K	153.6	162.5	34.3	56.1
L	153.0	161.8	33.1	47.3
M	154.3	162.1	30.5	37.3

CONCLUSIONS

1. This study investigated the potential use of and the combined effect of giant reed (GR) powder filler (10 wt% to 40 wt%) and nano-MgO (1 wt% to 2 wt%) on the water absorption, strength, and thermal properties of the recycled polypropylene (RPP) matrix. The addition of the GR filler resulted in a considerable improvement in the mechanical properties of the wood-polymer composites (WPCs), especially in the bending and tensile modulus while the water absorption increased.
2. The WPCs with the nano-MgO showed lower mechanical properties compared to the WPCs without the nano-MgO. Moreover, the addition of the nano-MgO increased the water absorption of the WPCs more than the WPCs without the nano-MgO. Increasing nano-MgO content improved the bending and tensile modulus, as well as the bending and tensile strength decreased.
3. The thermal studies indicated that the addition of the GR flour increased the thermal stability of the WPCs, while the addition of the nano-MgO decreased it.
4. When all the test results are evaluated, it can be said that the inclusion of 30 wt% GR flour in the RPP gave the best mechanical and thermal properties.

ACKNOWLEDGMENTS

This project was supported by Researchers Supporting Project Number RSP-2025R7 at King Saud University, Riyadh, Saudi Arabia.

Data Availability Statement

Data are available on request from the authors.

Declaration of Conflicting Interests

The authors declared no potential conflicts of interest with respect to the research, authorship, and/or publication of this article.

Funding

This work was financially supported by the Research Fund of Istanbul University-Cerrahpaşa, Project number: FYO-2021-35844.

REFERENCES CITED

- Adhikari, N. M., Tuladhar, A., Wang, Z., De Yoreo, J. J., and Rosso, K. M. (2021). “No hydrogen bonding between water and hydrophilic single crystal MgO surfaces?,” *The Journal of Physical Chemistry C* 125(47), 26132-26138. DOI: 10.1021/acs.jpcc.1c06486
- Alvarez, V. A., Ruscekaite, R. A., and Vazquez, A. (2003). “Mechanical properties and water absorption behavior of composites made from a biodegradable matrix and alkaline-treated sisal fibers,” *Journal of Composite Materials* 37(17), 1575-1588. DOI: 10.1177/0021998303035180
- Angelini, L. G., Ceccarini, L., Nasso, N., and Bonari, E. (2009). “Comparison of *Arundo donax* L. and *Miscanthus x giganteus* in a long-term field experiment in central Italy: analysis of productive characteristics and energy balance,” *Biomass and Bioenergy* 33, 635-643. DOI: 10.1016/j.biombioe.2008.10.005
- Arslan, M. B., and Şahin, H. T. (2014). “A study on alternative raw material source for giant reed (*Arundo donax* L.),” *Süleyman Demirel Üniversitesi Fen Bilimleri Enstitüsü Dergisi* 18(3), 90-96.
- Ayrilmis, N., and Ashori, A. (2014). “Lignocellulosic fibers and nanocellulose as reinforcing filler in thermoplastic composites,” *Eurasian Journal of Forest Science* 2(2), 1-6. DOI: 10.31195/ejejfs.70188
- Ayrilmis, N., Kanat, G., Yildiz Avsar, E., Palanisamy, S., and Ashori, A. (2024). “Utilizing waste manhole covers and fibreboard as reinforcing fillers for thermoplastic composites,” *Journal of Reinforced Plastics and Composites* 2024 (available online), article ID 07316844241238507. DOI: 10.1177/07316844241238507
- Ayrilmis, N., Kaymakci, A., and Ozdemir, F. (2013). “Physical, mechanical, and thermal properties of polypropylene composites filled with walnut shell flour,” *Journal of Industrial and Engineering Chemistry* 19(3), 908-914. DOI: 10.1016/j.jiec.2012.11.006
- Ayrilmis, N., Yurttas, E., Tetik, N., Özdemir, F., Palanisamy, S., Alagarsamy, A., Ramasamy, S., Sillanpää, M., and Al-Farraj, S. A. (2024). “Antibacterial performance of biodegradable polymer and hazelnut husk flour antibacterial biofilm with silver nanoparticles,” *BioResources* 19(4), 8812-8826. DOI: 10.15376/biores.19.4.8812-8826
- Basalp, D., Tihminlioglu, F., Sofuoglu, S. C., Inal, F., and Sofuoglu, A. (2020). “Utilization of municipal plastic and wood waste in industrial manufacturing of wood plastic composites,” *Waste and Biomass Valorization* 11, 5419-5430. DOI: 10.1007/s12649-020-00986-7
- Chaudemanche, S., Perrot, A., Pimbert, S., Lecompte, T., and Faure, F. (2018).

- “Properties of an industrial extruded HDPE-WPC: The effect of the size distribution of wood flour particles,” *Construction and Building Materials* 162, 543-552. DOI: 10.1016/j.conbuildmat.2017.12.061
- Chen, W.-H., Eng, C. F., Lin, Y.-Y., and Bach, Q.-V. (2020). “Independent parallel pyrolysis kinetics of cellulose, hemicelluloses and lignin at various heating rates analyzed by evolutionary computation,” *Energy Conversion and Management* 221, article ID 113165. DOI: 10.1016/j.enconman.2020.113165
- Črešnar, K. P., Plohl, O., and Zemljič, L. F. (2024). “Functionalised fibres as a coupling reinforcement agent in recycled polymer composites,” *Materials* 17(11), article 2739. DOI: 10.3390/ma17112739
- Díez, D., Urueña, A., Piñero, R., Barrio, A., and Tamminen, T. (2020). “Determination of hemicellulose, cellulose, and lignin content in different types of biomasses by thermogravimetric analysis and pseudocomponent kinetic model (TGA-PKM method),” *Processes* 8(9), article 1048. DOI: 10.3390/pr8091048
- Durmaz, S., Keles, O. O., Aras, U., Erdil, Y. Z., and Mengelöglu, F. (2023). “The effect of zinc oxide nanoparticles on the weathering performance of wood-plastic composites,” *Coloration Technology* 139(4), 430-440. DOI: 10.1111/cote.12666
- Ezzaraa, I., Ayrlimis, N., Abouelmajd, M., Kuzman, M. K., Bahlaoui, A., Arroub, I., Bengourram, J., Lagache, M., and Belhouideg, S. (2023). “Numerical modeling based on finite element analysis of 3D-printed wood-poly(lactic acid) composites: A comparison with experimental data,” *Forests* 14(1), article 95. DOI: 10.3390/f14010095
- Feng, L., and Xie, W. (2021). “Analysis of factors affecting creep of wood–plastic composites,” *Forests* 12(9), article 1146. DOI: 10.3390/f12091146
- Fiore, V., Botta, L., Scaffaro, R., Valenza, A., and Pirrotta, A. (2014). “PLA based biocomposites reinforced with *Arundo donax* fillers,” *Composites Science and Technology* 105, 110-117. DOI: 10.1016/j.compscitech.2014.10.005
- García-Ortuño, T., Andréu-Rodríguez, J., Ferrández-García, M. T., Ferrández-Villena, M., and Ferrández-García, C. E. (2011). “Evaluation of the physical and mechanical properties of particleboard made from giant reed (*Arundo donax* L.),” *BioResources* 6(1), 477-486. DOI: 10.15376/biores.6.1.477-486
- Gatou, M.-A., Skylla, E., Dourou, P., Pippa, N., Gazouli, M., Lagopati, N., and Pavlatou, E. A. (2024). “Magnesium oxide (MgO) nanoparticles: Synthetic strategies and biomedical applications,” *Crystals* 14(3), article 215. DOI: 10.3390/cryst14030215
- Hornak, J. (2021). “Synthesis, properties, and selected technical applications of magnesium oxide nanoparticles: A review,” *International Journal of Molecular Sciences* 22(23), article 12752. DOI: 10.3390/ijms222312752
- Huda, M. S., Drzal, L. T., Misra, M., Mohanty, A. K., Williams, K., and Mielewski, D. F. (2005). “A study on biocomposites from recycled newspaper fiber and poly (lactic acid),” *Industrial and Engineering Chemistry Research* 44(15), 5593-5601. DOI: 10.1021/ie0488849
- ISO 62 (2008). “Plastics – Determination of water absorption,” International Organization for Standardization, Geneva, Switzerland.
- ISO 178 (2010). “Plastics – Determination of flexural properties,” International Organization for Standardization, Geneva, Switzerland.
- ISO 180 (2019). “Plastics – Determination of Izod impact strength,” International Organization for Standardization, Geneva, Switzerland.
- ISO 291 (2008). “Plastics – Standard atmospheres for conditioning and

- testing,” International Organization for Standardization, Geneva, Switzerland.
- ISO 527-2 (2012). “Plastics – Determination of tensile properties – Part 2: Test conditions for moulding and extrusion plastics,” International Organization for Standardization, Geneva, Switzerland.
- Jusner, P., Schwaiger, E., Potthast, A., and Rosenau, T. (2021). “Thermal stability of cellulose insulation in electrical power transformers – A review,” *Carbohydrate Polymers* 252, article ID 117196. DOI: 10.1016/j.carbpol.2020.117196
- Karuppiyah, G., Kuttalam, K. C., and Palaniappan, M. (2020). “Multiobjective optimization of fabrication parameters of jute fiber / polyester composites with egg shell powder and nanoclay filler,” *Molecules* 25(23), article 5579. DOI: 10.3390/molecules25235579
- Kaymakçı, A., Ayırlmış, N., and Güleç, T. (2013). “Surface properties and hardness of polypropylene composites filled with sunflower stalk flour,” *BioResources* 8(1), 592-602. DOI: 10.15376/biores.8.1.592-602
- Kiaei, M., Moghdam, Y. R., Kord, B., and Samariha, A. (2017). “The effect of nano-MgO on the mechanical and flammability properties of hybrid nano composites from wood flour-polyethylene,” *Maderas. Ciencia y Tecnología* 19(4), 471-480. DOI: 10.4067/S0718-221X2017005000701
- Lazzeri, A., Zebarjad, S. M., Pracella, M., Cavalier, K., and Rosa, R. (2005). “Filler toughening of plastics. Part 1—The effect of surface interactions on physico-mechanical properties and rheological behaviour of ultrafine CaCO₃/HDPE nanocomposites,” *Polymer* 46(3), 827-844. DOI: 10.1016/j.polymer.2004.11.111
- Lewis, R., Weldekidan, H., Rodriguez, A. U., Mohanty, A. K., Mielewski, D. F., and Misra, M. (2023). “Design and engineering of sustainable biocomposites from ocean-recycled polypropylene-based polyolefins reinforced with almond shell and hull,” *Composites Part C: Open Access* 12, article ID 100373. DOI: 10.1016/j.jcomc.2023.100373
- Licursi, D., Antonetti, C., Bernardini, J., Cinelli, P., Coltelli, M. B., Lazzeri, A., Martinelli, M., and Galletti, A. M. R. (2015). “Characterization of the *Arundo donax* L. solid residue from hydrothermal conversion: Comparison with technical lignins and application perspectives,” *Industrial Crops and Products* 76, 1008-1024. DOI: 10.1016/j.indcrop.2015.08.007
- Lilholt, H., and Lawther, J. M. (2000). “Natural organic fibers,” *Comprehensive Composite Materials* 303-325. DOI: 10.1016/b0-08-042993-9/00048-6
- Mashkour, M., and Ranjbar, Y. (2018). “Superparamagnetic Fe₃O₄@ wood flour/polypropylene nanocomposites: Physical and mechanical properties,” *Industrial Crops and Products* 111, 47-54. DOI: 10.1016/j.indcrop.2017.09.068
- Meng, X., Hu, F., Liu, B., Cao, Y., Xu, H., Li, L., and Yu, L. (2023). “Study on the characterization of physical, mechanical, and mildew resistance properties of enzymatically treated bamboo fiber-reinforced polypropylene composites,” *Forests* 15(1), article 60. DOI: 10.3390/f15010060
- Monteiro, A., Teixeira, G., and Moreira, J. F. (2015). “Relationships between leaf anatomical features of *Arundo donax* and glyphosate efficacy,” *Revista de Ciências Agrárias* 38(2), 131-13
- Mylsamy, B., Shanmugam, S. K. M., Aruchamy, K., Palanisamy, S., Nagarajan, R., and Ayırlmış, N. (2024). “A review on natural fiber composites: Polymer matrices, fiber surface treatments, fabrication methods, properties, and applications,” *Polymer Engineering and Science* 64(6), 2345-2373. DOI: 10.1002/pen.26713

- Palaniappan, M., Palanisamy, S., Khan, R., H. Alrasheedi, N., Tadepalli, S., Murugesan, T. mani, and Santulli, C. (2024). "Synthesis and suitability characterization of microcrystalline cellulose from *Citrus x sinensis* sweet orange peel fruit waste-based biomass for polymer composite applications," *Journal of Polymer Research* 31(4), article 105. DOI: 10.1007/s10965-024-03946-0
- Palanisamy, S., Murugesan, T. M., Palaniappan, M., Santulli, C., Ayrlimis, N., and Alavudeen, A. (2024). "Selection and Processing of natural fibers and nanocellulose for biocomposite applications: A brief review," *BioResources* 19(1), 1789-1813. DOI: 10.15376/biores.19.1.Palanisamy
- Pan, P., Zhu, B., Kai, W., Serizawa, S., Iji, M., and Inoue, Y. (2007). "Crystallization behavior and mechanical properties of bio-based green composites based on poly (L-lactide) and kenaf fiber," *Journal of Applied Polymer Science* 105(3), 1511-1520. DOI: 10.1002/app.26407
- Plackett, D., Andersen, T. L., Pedersen, W. B., and Nielsen, L. (2003). "Biodegradable composites based on L-poly lactide and jute fibres," *Composites Science and Technology* 63(9), 1287-1296. DOI: 10.1016/S0266-3538(03)00100-3
- Ramos, D., El Mansouri, N.-E., Ferrando, F., and Salvadó, J. (2018). "All-lignocellulosic fiberboard from steam exploded *Arundo donax* L.," *Molecules* 23(9), article 2088. DOI: 10.3390/molecules23092088
- Shatalov, A. A., and Pereira, H. (2006). "Papermaking fibers from giant reed (*Arundo donax* L.) by advanced ecologically friendly pulping and bleaching technologies," *BioResources* 1(1), 45-61. DOI: 10.15376/biores.1.1.45-61
- Srivabut, C., Khamtree, S., Homkhiew, C., Ratanawilai, T., and Rawangwong, S. (2023). "Comparative effects of different coastal weathering on the thermal, physical, and mechanical properties of rubberwood–latex sludge flour reinforced with polypropylene hybrid composites," *Composites Part C: Open Access* 12, article ID 100383. DOI: 10.1016/j.jcomc.2023.100383
- Stokke, D. D., and Gardner, D. J. (2003). "Fundamental aspects of wood as a component of thermoplastic composites," *Journal of Vinyl and Additive Technology* 9(2), 96-104. DOI: 10.1002/vnl.10069
- Suárez, L., Castellano, J., Romero, F., Marrero, M. D., Benítez, A. N., and Ortega, Z. (2021). "Environmental hazards of giant reed (*Arundo donax* L.) in the Macaronesia region and its characterisation as a potential source for the production of natural fibre composites," *Polymers* 13(13), article 2101. DOI: 10.3390/polym13132101
- Suárez, L., Hanna, P. R., Ortega, Z., Barczewski, M., Kosmela, P., Millar, B., and Cunningham, E. (2024). "Influence of giant reed (*Arundo Donax* L.) culms processing procedure on physicochemical, rheological, and thermomechanical properties of polyethylene composites," *Journal of Natural Fibers* 21(1), article ID 2296909. DOI: 10.1080/15440478.2023.2296909
- Suárez, L., Ortega, Z., Romero, F., Paz, R., and Marrero, M. D. (2022). "Influence of giant reed fibers on mechanical, thermal, and disintegration behavior of rotomolded PLA and PE composites," *Journal of Polymers and the Environment* 30(11), 4848-4862. DOI: 10.1007/s10924-022-02542-x
- Sumesh, K. R., Palanisamy, S., Khan, T., Ajithram, A., and Ahmed, O. S. (2024). "Mechanical, morphological and wear resistance of natural fiber/glass fiber-based polymer composites," *BioResources* 19(2), 3271-3289. DOI: 10.15376/biores.19.2.3271-3289

Tisserat, B., Reifschneider, L., Núñez, J. C. L., Hughes, S. R., Selling, G., and Finkenstadt, V. L. (2014). "Evaluation of the mechanical and thermal properties of coffee tree wood flour-polypropylene composites," *BioResources* 9(3), 1-19. DOI: 10.15376/biores.9.3.1-19

Article submitted: November 12, 2024; Peer review completed: January 18, 2025;
Revised version received: January 22, 2025; Approved: February 5, 2025; Published:
February 17, 2025.

DOI: 10.15376/biores.20.2.2670-2686